Plant Molecular Biology (2022) 110:37–52
https://doi.org/10.1007/s11103-022-01282-9

Transcriptomic analysis reveals the role of FOUR LIPS in response to salt stress in rice

Chunxia Zhang[1] · Jie Zhang[1,2] · Huichao Liu[1,2] · Xiaoxiao Qu[1,2] · Junxue Wang[1,2,4] · Qixiumei He[1,2] · Junjie Zou[1,3] · Kezhen Yang[1] · Jie Le[1,2]

Received: 12 February 2022 / Accepted: 26 April 2022 / Published online: 18 May 2022

Abstract

Key message **An R2R3-MYB transcription factor FOUR LIPS associated with B-type Cyclin-Dependent Kinase 1;1 confers salt tolerance in rice.**

Abstract The Arabidopsis FOUR LIPS (AtFLP), an R2R3 MYB transcription factor, acts as an important stomatal development regulator. Only one orthologue protein of AtFLP, *Oryza sativa* FLP (OsFLP), was identified in rice. However, the function of OsFLP is largely unknown. In this study, we conducted RNA-seq and ChIP-seq to investigate the potential role of OsFLP in rice. Our results reveal that OsFLP is probably a multiple functional regulator involved in many biological processes in growth development and stress responses in rice. However, we mainly focus on the role of OsFLP in salt stress response. Consistently, phenotypic analysis under salt stress conditions showed that *osflp* exhibited significant sensitivity to salt stress, while *OsFLP* over-expression lines displayed obvious salt tolerance. Additionally, Yeast one-hybrid assay and electrophoretic mobility shift assay (EMSA) showed that OsFLP directly bound to the promoter region of *Oryza sativa* B-type Cyclin-Dependent Kinase 1;1 (*OsCDKB1;1*), and the expression of *OsCDKB1;1* was repressed in *osflp*. Disturbing the expression of *OsCDKB1;1* remarkably enhanced the tolerance to salt stress. Taken together, our findings reveal a crucial function of OsFLP regulating *OsCDKB1;1* in salt tolerance and largely extend the knowledge about the role of OsFLP in rice.

Keywords RNA-seq · ChIP-seq · *OsFLP* · *OsCDKB1;1* · Rice · Salt stress

Introduction

MYB (myeloblastosis) transcription factor genes family have a wide function in plant adaptive responses to adverse environment and growth development (El-Kereamy et al. 2012;

Chunxia Zhang and Jie Zhang have contributed equally to this work.

✉ Jie Le
lejie@ibcas.ac.cn

Chunxia Zhang
spring1984@163.com

Jie Zhang
jieer1027@163.com

Huichao Liu
liuhuichao@ibcas.ac.cn

Xiaoxiao Qu
quxiaoxiao721@sina.com

Junxue Wang
wangjunxues@163.com

Qixiumei He
heqixiumei@ibcas.ac.cn

Junjie Zou
zoujunjie@caas.cn

Kezhen Yang
ykzdsp@163.com

[1] Key Laboratory of Plant Molecular Physiology, CAS Center for Excellence in Molecular Plant Sciences, Institute of Botany, Chinese Academy of Sciences, Beijing 100093, China

[2] University of Chinese Academy of Sciences, Beijing 100049, China

[3] Biotechnology Research Institute, Chinese Academy of Agricultural Sciences, Beijing 100081, China

[4] Present Address: Wenbo School, Jinan 250100, China

Lv et al. 2017; Yang et al. 2012; Ye et al. 2015; Wang et al. 2021). MYB genes family are classified into four groups, including 1R-MYB, 2R-MYB, 3R-MYB, and 4R-MYB. Among them, R2R3-MYB genes are more prevalent in plants compared to those in animals (Martin and Paz-Ares 1997; Dubos et al. 2010). In Arabidopsis, FOUR LIPS (AtFLP) is an atypical R2R3-MYB transcription factor as a regulator in stomatal development (Yang and Sack 1995; Lai et al. 2005). Besides this, AtFLP/AtMYB88 play important role in abiotic stress responses (Xie et al. 2010b), root gravitropism by regulating the transcription of *PIN* genes (Wang et al. 2015), as well as regulating female reproductive development (Makkena et al. 2012). In addition, AtFLP/AtMYB88 are widely expressed in various tissues (Lei et al. 2015). These reports indicate that AtFLP serves as a pleiotropic regulator participating in several aspects of biological processes in Arabidopsis. Recently, the homolog of AtFLP in rice, OsFLP, was knocked out via the genome editing system. In contrast to the role in Arabidopsis, OsFLP is required for the proper orientation of symmetric division of guard mother cells (GMCs) in rice (Wu et al. 2019). However, little is known about the function of OsFLP and the downstream targets.

Salt stress as a crucial environmental factor affects plant growth and development and leads to reduce crop yield (Kreps et al. 2002; Gupta and Huang 2014; Roy et al. 2014; Zhang et al. 2022). To adapt to unfavorable environmental conditions, plants have evolved molecular mechanisms to protect themselves against stresses (Matsui et al. 2008). Thus, unraveling the salt stress-responsive mechanisms will be beneficial for improving plant salt tolerance and subsequently increasing crop production to ensure food security for the rapid growth of the global population. Salt stress causes several aspects of detrimental effects on plants. One of the most severe effects is the accumulation of Na^+ and Cl^-, which leads to ion imbalance and inhibits the uptake of K^+ resulting in reduced productivity and even death (James et al. 2011). Hence, maintaining Na^+/K^+ homeostasis in cells is vital for plants to survive under salt stress conditions. On the other hand, the production of ROS is enhanced and further leads to oxidative damages to the membranes, lipids, proteins (Mittler 2002). Many enzyme proteins such as superoxide dismutase (SOD), peroxidase (POD), catalase (CAT), glutathione peroxidase (GPX), ascorbate peroxidase (APX), are involved in ROS scavenging, and the activity of these proteins positively correlates with salt tolerance in plants (Mäkelä et al. 1999; Xia et al. 2014; Chen et al. 2021; Hasanuzzaman et al. 2021).

Besides *AtFLP/AtMYB88*, several genes have functions not only in controlling stomatal development but also in response to abiotic stress. For example, HIC, a negative regulator of stomatal development, controls stomatal density in response to elevated CO_2 (Gray et al. 2000). The cold-responsive gene *ICE1* participates in stomatal differentiation (Kanaoka et al. 2008). The *Arabidopsis* receptor-like kinase ERECTA (ER) controls stomatal patterning (Shpak et al. 2005). Over-expression of ER remarkably increased heat tolerance in plants (Shen et al. 2015a, b). Hence, these data implicate the cross-talk of the signal transduction pathways between stomatal development and abiotic stress.

Cyclin-dependent kinases (CDKs) mainly play roles in regulating cell division in plants (De Veylder et al. 2003; Dewitte and Murray 2003). In Arabidopsis, 12 CDKs have been identified with six categories (CDKA to CDKF) (Vandepoele et al. 2002). B-type CDKs including B1-type (CDKB1;1 and CDKB1;2) and B2-type (CDKB2;1 and CDKB2;2) subgroups are unique in plants (Vandepoele et al. 2002; Boudolf et al. 2001). In Arabidopsis, CDKB1;1 and CDKB1;2 act redundantly in regulating the symmetric division of GMCs. In addition, FLP/MYB88 could directly bind to the promoter region of *CDKB1;1* to regulate its expression during stomatal development (Xie et al. 2010a). Moreover, CDKB1;1 together with the RPA2a, which is a subunit of replication protein A complexes, restricts stomatal proliferation by CDKB1;1-mediated phosphorylation (Yang et al. 2019). OsCDKB1;1 could restore the impaired GMCs division and stomatal production in *Atcdkb1;1 1;2* mutants (Qu et al. 2018). In addition, salt stress affects the cell cycle regulation at the transcriptional level, ultimately leading to adaptive growth responses (Burssens et al. 2000). Salt stress responses involve the decline of cell cycle activity in the meristem of the root (West et al. 2004). However, the involvement of *OsCDKB1;1* in response to abiotic stress, especially salt stress, is still unknown yet.

In this study, we obtained an *osflp* mutant and generated the complemental transgenic lines. Using these materials, we performed the integrative analysis of RNA-seq and ChIP-seq. We found that the potential role of OsFLP was involved in several aspects of biological processes, especially in salt stress responses. *osflp* was more sensitive to salt stress with more ROS accumulation in plants compared with wild-type ZH11. Additionally, OsFLP could directly target the promoter region of *OsCDKB1;1* in vitro and repress its transcriptional expression. Consistently, *OsCDKB1;1*-RNAi plants exhibited significant salt tolerance with less ROS accumulation. Collectively, we conclude that upon salt stress, OsFLP represses the expression of *OsCDKB1;1* to confer salt tolerance in rice. These findings provide new functions of *OsCDKB1;1* out of cell cycle and novel insights into the role of OsFLP in rice.

Materials and methods

Plant materials and growth conditions

Rice, *Oryza sativa* L. ssp. *Japonica* cv. Zhonghua 11 (ZH11, wild type), were cultivated in the field of the Institute of

Botany, Chinese Academy of Sciences, Beijing, for propagating seeds.

Plant growth chambers were also used for rice cultivating with the following settings: 12 h day at 30 °C ± 2 °C, 12 h night at 22 °C ± 2 °C, and 60% humidity.

osflp mutant was obtained by TILLING (Targeting Induced Local Lesions IN Genomes) through an in-house TILLING platform (www.croptilling.org), which had a G→A point mutation in the sixth exon at the 2126 bp downstream of ATG position which led to the substitution of Ala with Thr. *osflp* mutants were identified by the observation of stomatal phenotype in leaves and confirmed by dCAP methods. The primers for dCAP were designed using the web site http://helix.wustl.edu/dcaps/dcaps.html. To obtain the *osflp* complementation line, 4733 bp genomic fragment of *OsFLP* was amplified and was sub-cloned into the destination vector pCAMBIA1301. The genomic region of *OsFLP* driven with the native promoter was introduced into the *osflp*. Several complementation lines were obtained and the abnormal GCs phenotype was rescued in these lines. One complementation line was used in this study and indicated as COM. For OsFLP over-expression lines, the sequence of the CDS was amplified and driven with 35S promoter. We selected the positive transgenic lines on MS solid medium supplemented with 25 μg/mL hygromycin.

To generate *OsFLP* and *OsCDKB1;1* over-expression line, full-length CDS fragments were amplified by PCR and were inserted into TOPO vector, followed by sub-cloning into pH7WG2D.1 vector via LR reaction of gateway cloning with 35S promoter. For making the GUS line, the promoter region of *OsFLP* was fused to the vector pGUS1301. These constructs were introduced into rice via an Agrobacterium-mediated transformation (Hiei et al. 1994). The homozygous lines were selected for further analysis.

Germination rates assay under salt stress

Salt tolerance phenotype assay was performed on half-strength Murashige & Skoog medium (MS) solid medium plates. Three-day-old rice seedlings grown on 1/2 MS solid medium vertical plates were transferred to new 1/2 MS solid medium on vertical plates supplemented with or without 200 mM NaCl. Pictures were taken 5 days after transfer.

Salt tolerance phenotype assay was performed with hydroponic culture. 14-day-old rice seedlings grown on 1/2 MS hydroponic culture were transferred to liquid medium supplemented with or without 150 mM NaCl for 3 days or 10 days, with intermittent changing of the liquid medium every 3 days. Finally the seedlings were transferred to fresh liquid medium for 3 days recovery.

Salt tolerance phenotype assay with rice seedlings were grown on soil. 14-day-old rice seedlings grown on 1/2 MS solid medium were transferred to soil for 1 week. After 1 week, watering was stopped for 1 week, followed by watering plants with tap water supplemented with or without 200 mM NaCl for 15 days and 21 days.

Survival rates and soluble sugar content measurement.

Survival rates were calculated after 21 days of salt stress treatment. No green shoots were counted as dead plants and the survival rate was shown as the percentage of alive seedlings.

Soluble sugar content was determined referring to the previous report (Tang et al. 2013). 500 mg leaves were ground in 2 mL 10% trichloroacetic acid (TCA), and the mixture was centrifuged at 4000 rpm for 10 min. 2 mL extracts were taken and equal volume of 0.6% thiobarbituric acid (TBA) was added. The mixture was incubated in boiled water for 15 min and quickly cooled on ice, and centrifuged at 4000 rpm for 15 min. The spectral absorbance of the supernatant was determined at 450 nm, 532 nm, and 600 nm with an ultraviolet spectrophotometer. Soluble concentration (mM) = 11.71 × D450.

SOD, POD, and CAT enzyme activities assays

500 mg rice leaves were ground with pre-cooled mortar and pestle in liquid nitrogen. Afterwards, 50 mM potassium phosphate buffer (pH 7.8) containing 1% polyvinylpyrrolidone was added and mixed thoroughly. Then the mixture was centrifuged at 15,000×*g* at 4 °C for 20 min. The supernatant was the crude enzyme extraction. The activities of SOD, POD, and CAT were determined following the previously described protocols (Miao et al. 2010). The final enzyme activities were calculated according to the following formulations. SOD activity (U/g min) = $(A_0 - A_S) \times V_t / (A_0 \times W \times 0.5 \times V_s)$, ($A_0$, absorbance value of the control; A_S, absorbance value of the samples; V_t, the total volume of the sample; W, the fresh weight of the sample; V_s, the volume of the sample for measurement). POD activity (U/g min) = $(\Delta A_{470} \times V_t) / (W \times V s \times 0.01 \times t)$, ($\Delta A_{470}$, the change of absorbance value at 470 nm wavelength per minute; V_t, the total volume of the sample; W, the fresh weight of the sample; V_s, the volume of the sample for measurement; t, interval time). CAT activity (U/g min) = $(\Delta A_{240} \times V_t) / (W \times Vs \times 0.1 \times t)$, $\Delta A_{240} = A_{S0} - (A_{S1} + A_{S2})/2$, ($\Delta A_{240}$, the change of absorbance value at 240 nm wavelength per minute; V_t, the total volume of the sample; W, the fresh weight of the sample; V_s, the volume of the sample for measurement; t, interval time; A_{S0}, absorbance value of the control; A_{S1} and A_{S2}, absorbance value of the samples).

Na^+ and K^+ content assay

Shoots and roots of rice seedlings were harvested separately. Samples were dried at 104 °C for 15 min and 55 °C for 3 days. Dry samples were digested in nitric acid overnight in dark and then transferred to 120 °C for 8–12 h. The content of Na^+ and K^+ in the extractions was measured with an ICP emission spectrometer (iCAP6300, Thermo scientific, US) according to the methods described previously (Shen et al. 2015b).

ROS content determination

The content of H_2O_2 was determined referring to the protocol described previously (Zhang et al. 2014). The commercial H_2O_2 detection kit (SolarBio Inc.) was used. In brief, approximately 100 mg rice leaves were ground with liquid nitrogen and 1 ml lysate buffer was added and mixed gently. The extraction was centrifuged at 8000×*g* for 10 min at 4 °C. The reaction buffer was added to the supernatant. Then mixed them gently, and reacted at room temperature for 5 min. The mixture was measured with an ultraviolet spectrophotometer at the 415 nm wavelength, and the H_2O_2 content was calculated according to the formulation in the manufacturer's protocol. We also used 3,3-diaminobenzidine (DAB) staining for the detection of H_2O_2 and nitroblue tetrazolium (NBT) staining to determine O_2^- according to the previously described protocol (Zhang et al. 2014a). In brief, for the DAB staining assay, the rice leaves were cut into around 1 cm length, immersed in 1 mg/mL DAB solution, incubated at room temperature for 8 h. Afterwards, samples were transferred into ethanol to remove the chlorophyll heating with water bath at 100 °C for 2 h. For NBT staining assay, around 1 cm length of rice leaves was immersed in 6 mM NBT solution and incubated at room temperature for 8 h. Ethanol was used to remove the chlorophyll and pictures were taken for analysis.

Yeast one-hybrid assay

In yeast one-hybrid assay, the activated domain AD vector and the LacZ reporter BD vector were used. *OsFLP* was fused to the AD vector (*OsFLP*-AD). The 2266 bp promoter of *OsCDKB1;1* was truncated into nine fragments (− 2266 to − 1132 bp, − 2266 to − 1683 bp, − 1701 to − 1132 bp, − 1208 to − 537 bp, − 632 to − 1 bp, − 536 to − 413 bp, − 418 to − 275 bp, − 274 to − 138 bp, − 137 to − 1 bp), and fused with LacZ reporter BD vector, respectively. Afterwards, the fused AD and BD vectors were co-transformed into the EGY48 yeast strain and performed X-gal staining.

RNA-sequencing, ChIP-sequencing, and RT-qPCR analysis

For RNA-sequencing analysis, ZH11 and *osflp* mutant plants were grown under 30 °C ± 2 °C, 12 h day/22 °C ± 2 °C, 12 h night conditions for 7 days. The shoots of the seedlings were harvested and frozen in liquid nitrogen. RNA was extracted with TRIzol reagent (Invitrogen). The libraries were sequenced based on the Illumina platform and were performed by BioMarker Inc (Beijing, China). The clean reads were used for the subsequent analysis. Genes with adjusted p-value < 0.05 and log2 fold-change > 1 were taken as the differential expressed genes (DEGs). The GO enrichment of DEGs analysis was conducted with AgriGO V2.0 (http://systemsbiology.cau.edu.cn/agriGOv2/).

To generate *OsFLP:gOsFLP*-MYC plants, the genomic sequence of *OsFLP* was amplified with the gOsFLP-F primer (ATGGCGACCGGACCGATCT) and gOsFLP-R primer (AAGCTTTTATACCGAGTTCAAGTCT), and sub-cloned into a pSUPER:1300-MYC vector driven with OsFLP native promoter. Chromatin immunoprecipitation (ChIP) was performed with 7-day-old rice seedlings. The sequencing was performed by Wuhan Igenebook Biotechnology Co., Ltd (Wuhan, China).

For RT-qPCR analysis, RNA was extracted with HiPure Plant RNA Mini Kit (Angen Biotech CO., Ltd). The first-strand cDNA was synthesized with a PrimeScript® RT Reagent Kit (Takara). Real-time PCR was performed in a 96-well plate with the LightCycler96 system. Each reaction with 20 µl final volume contained the following ingredients: 10 µl Hieff® qPCR SYBR® Green Master Mix (No Rox), 0.8 µl gene-specific primers (10 µM), 2 µl cDNA which had been diluted 10 times from the original cDNA solution. Three steps amplification program was used as follows: 95 °C for 5 min, 40 cycles with 95 °C for 10 s, 55 °C for 20 s, and 72 °C for 20 s, finally following with melting curve step. *OsACT1* was used as the internal reference gene for normalization. The primers are listed in supplementary table S3.

Electrophoretic mobility shift assays (EMSA)

The coding sequence of *OsFLP* was amplified by PCR inserted into the pET28a vector and transformed into *E. coli* DE3 (BL21) cells for expressing the recombinant protein. The OsFLP protein was purified with His tag (Wang et al. 2015). Oligonucleotide probes were synthesized and labeled with Biotin 3′ End DNA Labeling Kit (PIERCE). For EMSA assay, 20 µL volume of reactions included the following components: His-OsFLP recombinant protein, labeled probes, 10 × binding buffer, 100 mM $MgCl_2$, 50% (v/v) glycerol, 1 µg/µL poly (dI-dC), and 1% (v/v) Nonidet P–40. Unlabeled probes were added for the competition assay. The

reaction was incubated at room temperature for 20 min. The reaction mixtures were analyzed by electrophoresis. The LightShift Chemiluminescent EMSA kit (Thermo Scientific, 20,148) was used to detect the Biotin-labeled probes.

Statistical analysis

The significant differences were analyzed by Student's *t* test. $P < 0.05$ and $P < 0.01$ were taken as statistically significant differences and were indicated with "*" and "**", respectively.

Accession numbers

Sequences used in this study were download from the Rice Genome Annotation Project Database (http://rice.plantbiology.msu.edu/) with the following accession numbers: *OsFLP* LOC_Os07g43420*; OsCDKB1;1* LOC_Os01g67160*; OsPRX107* LOC_Os07g44550*; OsPRX109* LOC_Os07g47990; *OsPRX112* LOC_Os07g48030*; OsMSA* LOC_Os04g10010; *OsPP2C* LOC_Os01g62760; *OsPRX72* LOC_Os05g06970; *OsPRX56* LOC_Os04g53630; *OsPRX87* LOC_Os06g35490; *OsPRX34* LOC_Os03g02939; LOC_Os05g06750; *OsRab16A* LOC_Os02g04680*; OsNAC5* LOC_Os07g37920*; OsDREB2A* LOC_Os01g07120*; OsDREB1F* LOC_Os01g73770*; OsACTIN2* LOC_Os03g50885.

Results

The phylogenetic relationship analysis of FLP in plants

The FLP encodes an R2R3-MYB transcription factor protein (Lai et al. 2005; Wu et al. 2019). To explore the evolutionary relationship of the FLP in different species, including algae, lower plants, and higher plants, we conducted phylogenetic tree analysis with OsFLP amino acids as a probe (Fig. S1). The results revealed that FLP is present in both monocots and dicots. It indicates that the function of FLP is conserved in plants. In most cases only one copy of FLP is available in monocots, however, two copies of FLP usually appeared in dicots. For example, in Arabidopsis, FLP and its paralogue MYB88 play a different but complementary role in regulating primary and lateral root gravitropism. However, in rice genome, only one OsFLP is found. It is speculated that OsFLP may be a pleiotropic regulator in rice. Taken together, it seems likely that in monocots, FLP acts as a pleiotropic regulator, while in dicots, FLP and its paralogs complementarily participate in regulating development and responses in plants.

The OsFLP orthologous proteins were not only present in higher plants (*Panicum miliaceum*, *Brachypodium distachyon, Setaria viridis, Setaria italic*, *Zea mays, Sorghum bicolor, Oryza sativa, Arabidopsis thaliana, Glycine max, Medicago truncatula, and Medicago sativa*) with stomata but also in the lower plants (*Zostera marina*) without stomata, even in the single-cell green algae (*Coccomyxa subellipsoidea* and *Chlamydomonas reinhardtii*) (Fig. S1). Thus, these data indicate that besides the function in regulating stomatal development, FLP may be also involved in other functions in plant development or adaptation to unfavorable environmental conditions.

Transcriptomic analysis of the *osflp* mutant

To facilitate functional analysis of OsFLP, we obtained an *osflp* mutant line based on TILLING system. The substitution of Ala with Thr in the sixth exon in *osflp* mutant led to the abnormal GCs development in leaves. In *osflp*, after cell division of GMCs, the orientation of the cell plate was misplaced in multiple orientation and the formation of the pore between the guard cells was impaired. The complementary line (COM) could rescue the phenotype. (Fig. 1A–E). This phenotype is consistent with the previous report on *osflp* with T-DNA insertion (Wu et al. 2019).

To explore the potential functions of OsFLP, we performed the RNA-sequencing (RNA-seq) analysis with the shoots of 7-day-old seedlings of *osflp* and the wild-type ZH11 under normal growth condition.In total, we identified 755 differentially expressed genes (DEGs), including 328 up-regulated genes and 427 down-regulated genes in *osflp* compared with ZH11 (Fig. 2A, Dataset S1). In these DEGs, several types of genes might be regulated by OsFLP including "transcription factors" "transferase proteins" "cell wall-related genes" "environmental stress-responsive genes" "metabolism pathway" and "hormone-related genes", etc. (Fig. 2B, Dataset S2). These results indicate that OsFLP may be involved in various aspects of plant development and environmental stress responses.

To further unravel the function of OsFLP, we performed Gene Ontology (GO) analysis with up-regulated and down-regulated DEGs, respectively. Intriguingly, GO analysis revealed that GO terms related to peroxidase activity, oxidative stress reactive oxygen species metabolic process, and so on were significantly enriched with down-regulated DEGs other than up-regulated DEGs (Fig. 2C, Dataset S3). Several class III peroxidases (PRXs) were identified according to the GO terms and most of these PRXs were downregulated in *osflp* (Supplementary Table S1). Furthermore, to confirm the RNA-seq data, the expression of ten randomly selected genes was detected by RT-qPCR. The results are consistent with RNA-seq (Supplementary Fig. S2A, B). Considering PRXs responsible for H_2O_2 metabolism (Almagro et al.

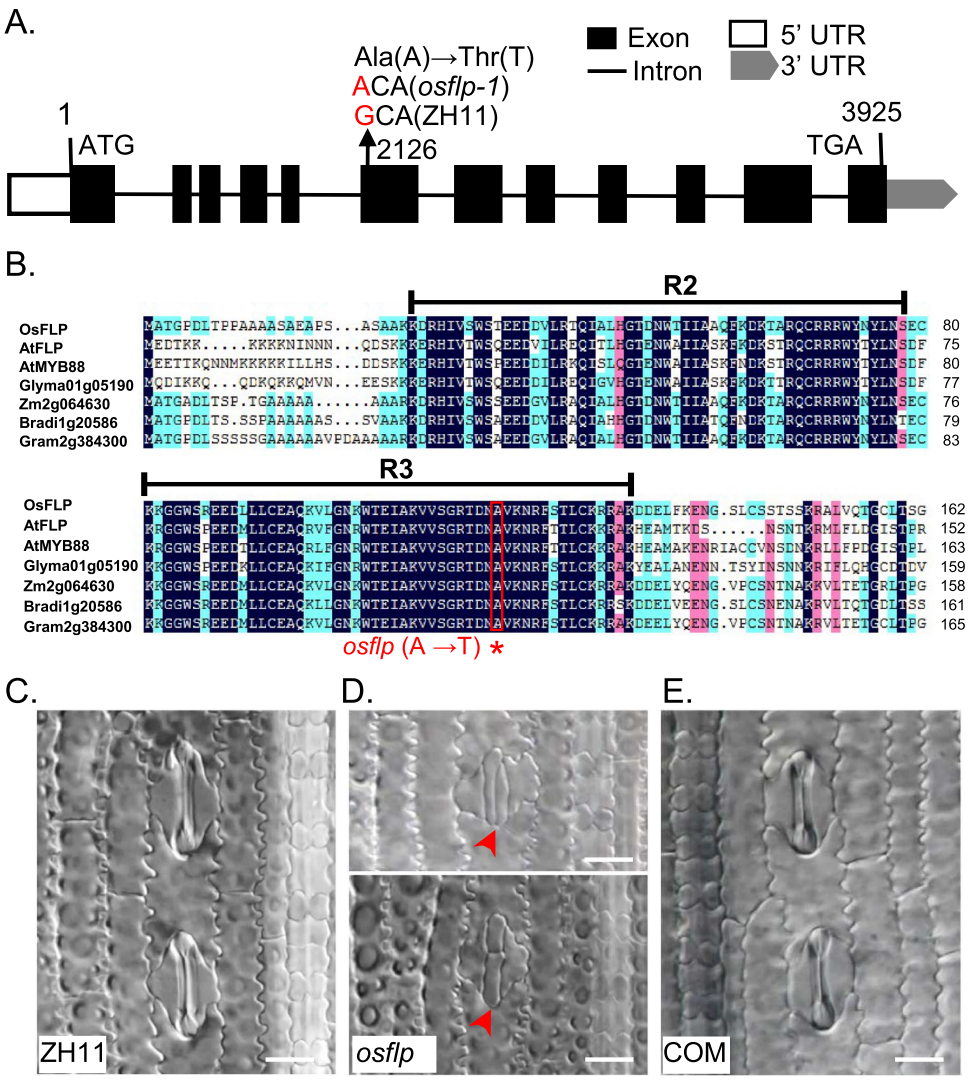

Fig. 1 The characterization of *osflp*. **A** *osflp* mutant line was obtained by TILLING system. A point mutation nucleotide G to A was identified in the sixth exon at position 2126 bp downstream of ATG which led to the substitution of amino acid Ala with Thr. **B** Multiple alignments of amino acid sequences of OsFLP, AtFLP, AtMYB88, Glyma01g05190, Zm24064630, Bradi1g20586, Gram2g384300, showed the mutation site of *osflp* located in the highly conserved region of R3 domain. **C–E**. Normal stomata in ZH11 and complementation line. Abnormal division and differentiation stomata in *osflp* were indicated with red arrowhead, Scale bars = 20 μm

2009), OsFLP may play a role in controlling ROS-related pathways. Thus, the expression of Os*POD1*, Os*POD2,* and *OsCAT*, which are involved in ROS scavenging (Miller et al. 2010; Mittler 2002; Noctor and Foyer 1998), were detected. The results showed that the expression of three genes significantly decreased in *osflp* compared with ZH11 (Supplementary Fig. S2C).

To further identify the direct targets of OsFLP, the ChIP-seq analysis was conducted with *pOsFLP::OsFLP-MYC* in *osflp*. After removal of the background peaks, a total of 12,899 peaks were identified (Dataset S4). KEGG pathway analysis showed that the potential direct targets of OsFLP related to various pathways, including "spliceosome", "mRNA surveillance pathway", "N-Glycan biosynthesis", "endocytosis", "RNA transport" and "oxidative phosphorylation", etc. (Fig. 2D, Dataset S5). Among them, oxidative phosphorylation is closely related to ROS metabolism.

Through the integrative analysis of RNA-seq data and ChIP-seq data, 125 genes were found to be present in both RNA-seq and ChIP-seq profiles (Fig. 2E, Dataset S6). KEGG pathway analysis showed that peroxisome related pathway was included (Supplementary Fig. S3, Dataset S7). Peroxisome mainly controlling ROS scavenging was enriched. This result implied that OsFLP may play a role in ROS metabolism.

In addition, 10 genes out of 125 genes were related to salt stress responses, Na^+ and K^+ transports, as well as oxidoreductase activity (Supplementary Table S2). In addition, to further confirm the salt stress-responsive function of *OsFLP*, the expression levels of four salt stress-responsive genes including *OsRab16A, OsNAC5, OsDREB2A, and OsDREB1F* (Song et al. 2011; Ponce et al. 2021; Yang et al. 2012), were examined in ZH11, *osflp*, COM, and OE with or without NaCl stress. With salt stress conditions, the expression of these four genes significantly decreased in *osflp*, whereas increased in OE, compared with ZH11 and COM in rice (Fig. 2F–I). Taken together, these data show that OsFLP affects the expression of salt stress-responsive

genes as well as the ROS metabolic genes, suggesting the possible involvement of OsFLP in salt stress responses.

OsFLP plays a vital role in response to salt stress

To verify the role of OsFLP in response to salt stress, the expression pattern of *OsFLP* under salt stress was determined. The expression of *OsFLP* was increased after 2 h salt stress treatment and reached the maximal level after 6 h salt stress treatment (Supplementary Fig. S4A). Consistently, the shoots and leaves of the *pOsFLP*::GUS transgenic plants also showed increased GUS activity after 6 h salt stress treatment (Supplementary Fig. S4B).

The increased expression of *OsFLP* induced by salt stress encouraged us to examine the phenotype of *osflp* under salt stress conditions. Upon 150 mM NaCl stress, the germination rate of ZH11 and COM were almost 100%, while in *osflp,* it was much lower, around 53% after 5 days (Supplementary Fig. S5A–C). Furthermore, under 200 mM NaCl stress condition, compared to ZH11 and COM, *osflp* had shorter roots and shoots. In contrast, significant increases in shoot and root length were observed in the *OsFLP* overexpression plants (OE) (Fig. 3A–C). To further confirm the salt responsive function of *OsFLP*, we performed the phenotypic analysis with plants cultivated in soil. Three-week-old seedlings were treated with 200 mM NaCl for 15 days and 21 days, respectively. *osflp* exhibited more sensitivity with the significantly decreased survival rate (about 18.75%) compared with ZH11(about 87.5%), and COM plants could completely rescue the salt-sensitive phenotype with around 81.25% of plants survival rate, whereas OE plants behaved more resistance to salt stress with 100% survival rate (Fig. 3D, E). Taken together, these data indicate that OsFLP serves as a positive regulator in salt stress response in rice.

osflp accumulates more ROS under salt stress conditions

Salt stress usually causes ROS accumulation in plants (Xiong et al. 2002; Yang and Guo 2018). A high concentration of ROS leads to oxidative damage to membranes (lipid peroxidation), proteins, RNA, and DNA molecules (Mittler 2002). Several enzymes such as superoxide (SOD), peroxidase (POD), and catalase (CAT) contribute to the ROS detoxification in plants (Mittler et al. 2004). Our transcriptomic analysis showed that many genes, involved in ROS metabolism, were enriched (Fig. 2C). Hence, we investigated if ROS homeostasis was affected in *osflp* and OE plants under salt stress conditions. Considering hydroponic cultivation is more stable and easier for stress treatment, we performed the following measurements with hydroponic cultivation. Different from MS solid medium, 200 mM NaCl is too high to survive for most seedlings growing in hydroponic culture, so the concentration of NaCl was adjusted to 150 mM. Two-week-old seedlings of ZH11, *osflp*, COM, and OE were treated with or without 150 mM NaCl for 3 days and 10 days, respectively, afterward following 3 days recovery (Fig. 4A). Salt stress generally increased soluble sugar concentration (Dubey and Singh 1999). Thus, we performed measurements with survival rate and the soluble sugar content. It showed that the survival rate and the soluble sugar content were significantly lower in *osflp* but higher in OE plants, compared with ZH11 and COM under salt stress (Fig. 4B, C). Then, we checked the enzyme activities of SOD, POD, and CAT in ZH11, *osflp*, OE, and COM. Under non-salt treatment conditions, the activities of these enzymes in *osflp* and OE were very similar to those in ZH11 and COM. However, upon salt stress, the activities of these enzymes significantly reduced in *osflp* but enhanced in OE (Fig. 4D–F). In addition, with salt treatment conditions, more H_2O_2 accumulated in *osflp* but less in OE (Fig. 4G). Consistently, diaminobenzidine (DAB) and nitro blue tetrazolium (NBT) staining also confirmed the higher contents of ROS in *osflp* relative to ZH11 and COM (Fig. 4H, I). Collectively, these results suggest that OsFLP affects ROS accumulation in response to salt stress.

OsFLP confers salt tolerance by reducing sodium accumulation

Under salt stress conditions, intracellular Na^+ and K^+ homeostasis is essential for cell activities and is crucial for salt tolerance in plants (Zhu 2003; Horie et al. 2001). To test if Na^+ and K^+ homeostasis was changed in *osflp* mutant and OE lines with salt stress, we measured Na^+ and K^+ contents in both shoots and roots. Under normal growth conditions, no significant differences in Na^+ and K^+ contents were observed in both *osflp* and OE lines compared to ZH11 and COM. However, with 150 mM NaCl treatment, Na^+ contents were significantly higher in both shoots and roots of *osflp* mutant compared to ZH11 and COM. In contrast, in OE lines, Na^+ contents were much lower in both shoots and roots (Fig. 5A, D). Whereas, K^+ contents behaved oppositely (Fig. 5B, E). Thus, with NaCl treatment, the ratio of Na^+/K^+ in both shoots and roots was increased in *osflp* and decreased in OE plants (Fig. 5C, F). This result indicated that the excessive Na^+ was accumulated in *osflp* under salt stress condition.

OsCDKB1;1 is the direct target of OsFLP

In Arabidopsis, AtFLP/AtMYB88 directly controlled *AtCDKB1;1* expression to regulate symmetric division in stomatal development (Xie et al. 2010a). OsCDKB1;1 shares 88.5% amino acid identity with *AtCDKB1;1* and *AtCDKB1;2* (Qu et al. 2018). To identify the target of

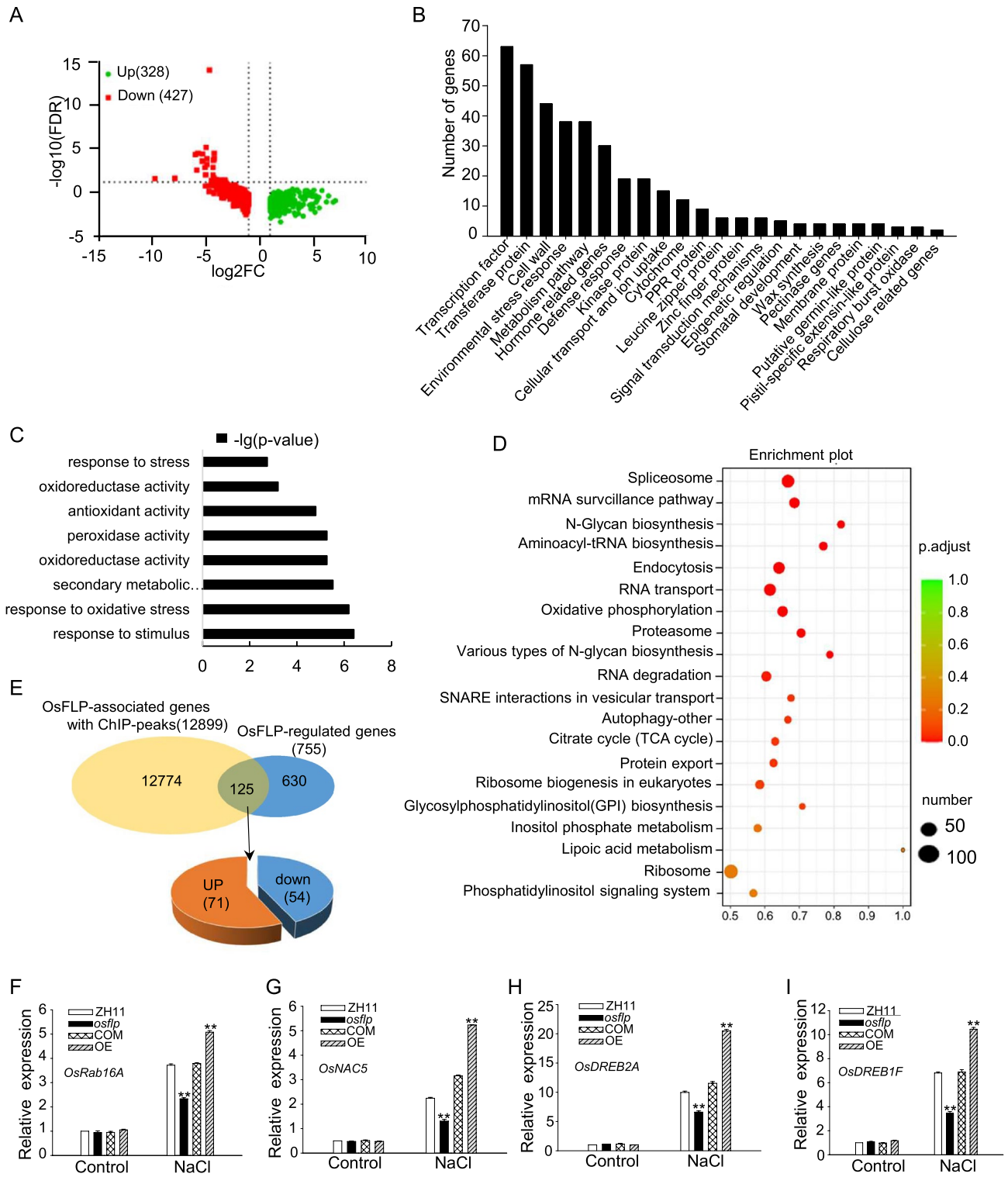

OsFLP, *OsCDKB1;1* was taken as one potential candidate. The expression of *OsCDKB1;1* was significantly induced in *osflp* but repressed in OE, compared with that in ZH11 and COM (Fig. 6A), suggesting that OsFLP negatively regulates the transcriptional expression of *OsCDKB1;1*. To examine whether OsFLP can directly bind to the promoter region of *OsCDKB1;1*, yeast one-hybrid assays were conducted. The 2266 bp upstream of the transcriptional start site (ATG) was truncated into several fragments. The results showed that OsFLP is directly bound to the region of 137 bp upstream of ATG, but not to the other regions of *OsCDKB1;1* promoter (Fig. 6B). AtFLP could bind DNA containing the core

◂**Fig. 2** Identification of potential targets of OsFLP by transcriptomic analysis. **A** Volcano Plot shows the up-and down-regulated genes in *osflp* mutant compared with ZH11. **B** The potential proteins or biological processes which are related to OsFLP, are identified by RNA-seq analysis. **C** GO term enrichment of differentially expressed genes (DEGs) for biological process with RNA-seq analysis. **D** KEGG enrichment analysis with ChIP-seq. Several potential pathways were enriched with KEGG analysis, including "spliceosome", "mRNA surveillance pathway", "N-Glycan biosynthesis", "endocytosis", "RNA transport" and "oxidative phosphorylation" etc. **E** The integrative of RNA-seq and ChIP-seq. In total, 125 genes were identified as the potential targets of OsFLP. Among them, 71 genes were induced and 54 genes were repressed. **F–I** The expression of salt stress-related genes *OsRab16A*, *OsNAC5*, *OsDREB2A*, *OsDREB1F* were detected using RT-qPCR with or without salt treatment in ZH11, *osflp*, COM and OE lines, respectively. *OsActin* was always taken as the reference gene. Data are means ± SD. The student's *t-test* was performed. Statistically significant differences are indicated with asterisks: $*P < 0.05$, $**P < 0.01$

consensus sequence [A/T/G] [A/T/G]C[C/G] [C/G] (Xie et al. 2010a). In our ChIP-seq data, a similar motif was identified for OsFLP in Fig. 6C. To determine the exact sequence which was bound by OsFLP, we scanned the *OsCDKB1;1* promoter region 137 bp upstream of ATG (− 137 to − 1 bp) and found six potential binding sites including − 130 to − 126 bp (TTCCC), − 125 to − 121 bp (TTCCC), − 114 to − 110 bp (ATCCC), − 78 to − 74 bp (ATCCC), − 18 to − 14 bp (ATCGG) and − 10 to − 6 bp (TTCGG) (Fig. 6D). To confirm the binding specificity, we truncated this 137 bp promoter region into three fragments with − 137 to − 95 bp, − 95 to − 45 bp and − 45 to − 1 bp, respectively, and performed electrophoretic mobility shift assay (EMSA) using recombinant OsFLP. Ultimately, we found that − 125 to − 121 bp (TTCCC) and − 78 to − 74 bp (ATCCC) were required for OsFLP binding with obviously shifted bands. By contrast, the mutant versions and the excess of the unlabeled probe as competitors, failed to form the shifted bands (Fig. 6E–G).

OsCDKB1;1 negatively regulates salt stress responses

As the expression of *OsCDKB1;1* was directly regulated by OsFLP (Fig. 6A), we were wondering if *OsCDKB1;1* was also involved in the salt stress responses in rice. Then, we were encouraged to examine whether *OsCDKB1;1* was required for salt tolerance. We exposed 2-week-old seedlings of *OsCDKB1;1* over-expression plant (*OsCDKB1;1*-OE) and the *OsCDKB1;1* knockdown plant (*OsCDKB1;1*-RNAi) (Qu et al. 2018) to150 mM NaCl stress condition, with ZH11 as control. After 12 days of salt stress and 3 days recovery, *OsCDKB1;1*–OE plants exhibited more sensitivity to salt stress, while *OsCDKB1;1*-RNAi behaved more tolerance to salt stress compared with ZH11 (Fig. 7A). Consistently, under salt stresses, the survival rate was significantly lower in *OsCDKB1;1*–OE plants but much higher in *OsCDKB1;1*-RNAi plants compared with ZH11 (Fig. 7B). It suggested that *OsCDKB1;1* had a negative function on salt stress tolerance in rice.

To investigate whether the ROS accumulation was impacted in *OsCDKB1;1*-RNAi plants, we measured the H_2O_2 content with or without salt stress. Intriguingly, upon salt stress, compared with ZH11, a higher level of H_2O_2 was accumulated in *OsCDKB1;1*–OE plants, while the lower level of H_2O_2 was accumulated in *OsCDKB1;1*-RNAi plants (Fig. 7C), suggesting that *OsCDKB1;1* influenced the content of H_2O_2 under salt stress condition. Collectively, these results indicate that *OsCDKB1;1* plays a negative role in response to salt stress by increasing ROS production.

Discussion

AtFLP as a pleiotropic regulator involves in several aspects of plant physiological processes, including stomatal development, abiotic stress response, root gravitropism, and female reproductive development (Xie et al. 2010a, 2010b; Wang et al. 2015; Makkena et al. 2012). In rice, it has been reported that OsFLP controls the orientation of the GMC symmetric division in stomatal development (Wu et al. 2019), but the downstream targets are unknown. Our phylogenetic tress analysis shows that the function of FLP is conserved and divergent in monocots and dicots plants (Fig. S1). However, the function of OsFLP in rice is still largely unknown. In this study, transcriptomic analysis indicated that the role of OsFLP was involved in many aspects, while we mainly focused on the salt stress responses. We also found that the *osflp* mutant was sensitive to salt stress with more ROS accumulation but the OE lines behaved conversely. It indicates that OsFLP acts as a key regulator in salt tolerance in rice.

The Na^+/K^+ ratio in the cytosol is important for keeping the normal cellular activities in plants. Under salt stress conditions, the uptake of Na^+ competes with K^+ and even the salt stress blocks the K^+ specific transporters (Zhu 2003). Our findings showed that more Na^+ was taken up into the cells of *osflp* under salt stress conditions. In this process, some sodium transporters may be involved (Fig. 7D). Interestingly, the integrative analysis of RNA-seq and ChIP-seq identified the Ca^{2+}/Na^+ antiporter (Os03g0411300) with increased expression, and the potassium channel (Os01g0846300) with decreased expression (Supplementary Table S2). Hence, we proposed that OsFLP may regulate the activity of Ca^{2+}/Na^+ antiporter and potassium channels to control the intracellular concentration of Na^+. In Arabidopsis, AtFLP together with *AtCDKB1;1* and *AtCDKB1;2* controls the stomatal division. However, in rice, no obvious phenotype in stomatal development in *oscdkb1;1* was

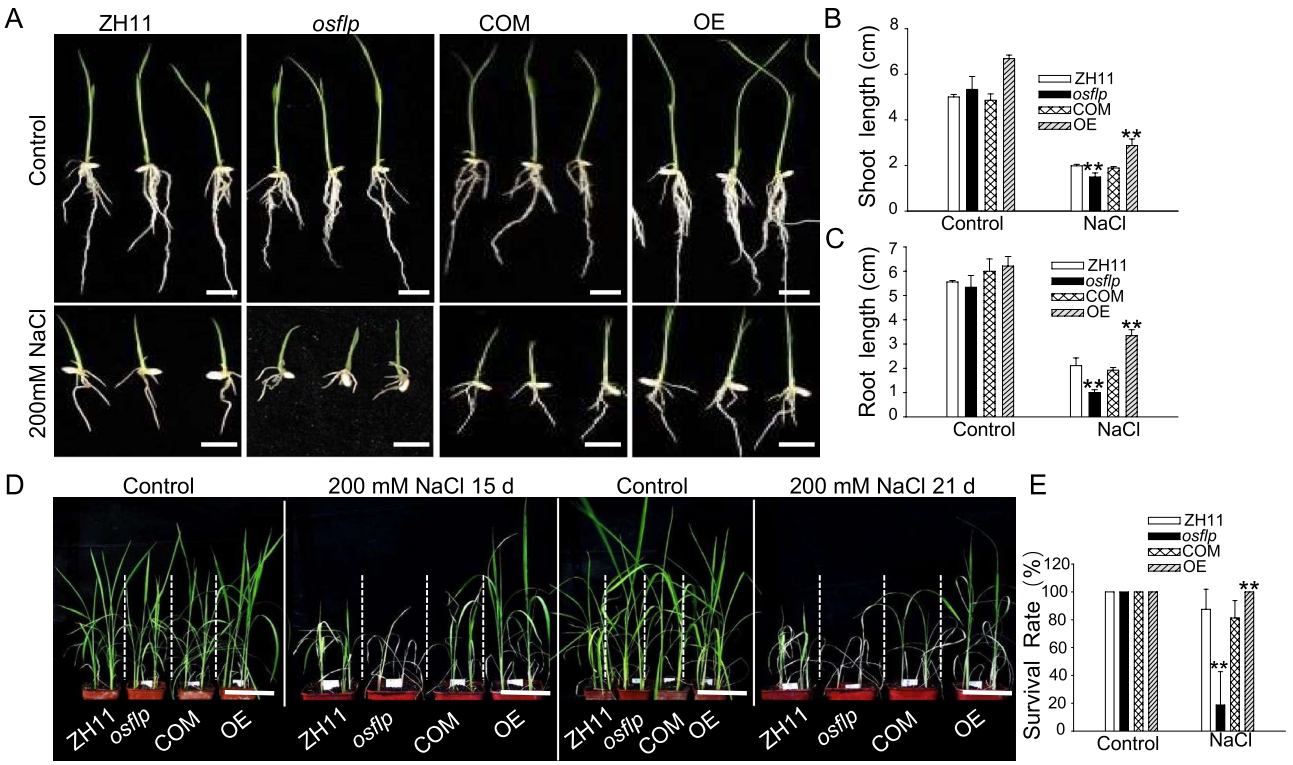

Fig. 3 *osflp* mutants are more sensitive to salt stress. **A** Salt stress tolerance phenotype assay of ZH11, *osflp*, COM and OsFLP overexpression line (OE) seedlings with or without NaCl treatment. Seedlings were grown on 1/2 MS plates for 3 days and transferred to 1/2 MS plates supplemented with or without 200 mM NaCl for 5 days. Scale bars = 1 cm. **B** and **C** The root length and the shoot length of ZH11, *osflp*, COM and OE seedlings were quantified, respectively, in D. Data are means ± SD. The student's *t-test* was performed. Statistically significant differences are indicated with asterisks: $^{**}P < 0.01$. **D** Salt stress tolerance phenotype assay of ZH11, *osflp*, COM, and OE seedlings were grown on soil. 7-day-old seedlings cultivated on soil were irrigated either with water or water supplement with 200 mM NaCl for 15 days and 21 days, respectively. Scale bars = 10 cm. **E** Survival rates of ZH11, *osflp*, COM, and OE plants after 21 days of stress treatment were analyzed. Data are means ± SD. The student's *t-test* was performed. Statistically, significant differences are indicated with asterisks: $^{**}P < 0.01$

observed (Qu et al. 2018; Menges et al. 2005; Porceddu et al. 2001; Andersen et al. 2008). However, in Arabidopsis, the response to salt stress involves a rapid decline of cell cycle activity (Burssens et al. 2000; West et al. 2004), and the expression of CDKB1;1 and CDKB1;2 was downregulated under salt stress (Mahapatra and Roy 2021). Intriguingly, in our findings, *oscdkb1;1* exhibited significantly salt tolerance with less ROS accumulation under salt stress conditions, suggesting that *OsCDKB1;1* had a negative function in salt stress response. Considering OsFLP directly binding to the promoter region of *OsCDKB1;1* and repressing its transcription, we conclude that OsFLP associated with *OsCDKB1;1* confers salt tolerance in rice. Thus, our findings uncover a novel OsFLP-*OsCDKB1;1* module conferring salt tolerance by involving ROS accumulation in rice.

Many PRXs genes were identified in *osflp* by RNA-seq analysis. PRXs paly important role in in catalyzing ROS scavenging (Bhatt and Tripathi 2011; Almagro et al. 2009), indicating that OsFLP might directly or indirectly regulate PRXs to influence the ROS contents in plants. Hence, in the future, it will be interesting to explore how OsFLP mediates the transcription of PRXs to affect the ROS accumulation. The root development plasticity is a hallmark of plant's response to salt stress (Koevoets et al. 2016). The transport of auxin is vital for the maintenance of the local level of auxin, which is dispensable for root growth and development (Korver et al. 2018). The root of *osflp* is more sensitive to salt stress compared with ZH11 and the over-expression lines (Fig. 3A). In Arabidopsis, AtFLP and its paralog MYB88 affect root gravitropism by regulating the transcription of *PIN3* and *PIN7* which are responsible for auxin transport (Wang et al. 2015). In rice, whether OsFLP is related to auxin transportation to control root development under salt stress conditions, it is worth verifying in the future.

Based on our findings, we proposed a working model for OsFLP-*OsCDKB1;1* mediated salt tolerance in rice (Fig. 7D). Under salt stress conditions, in ZH11, OsFLP

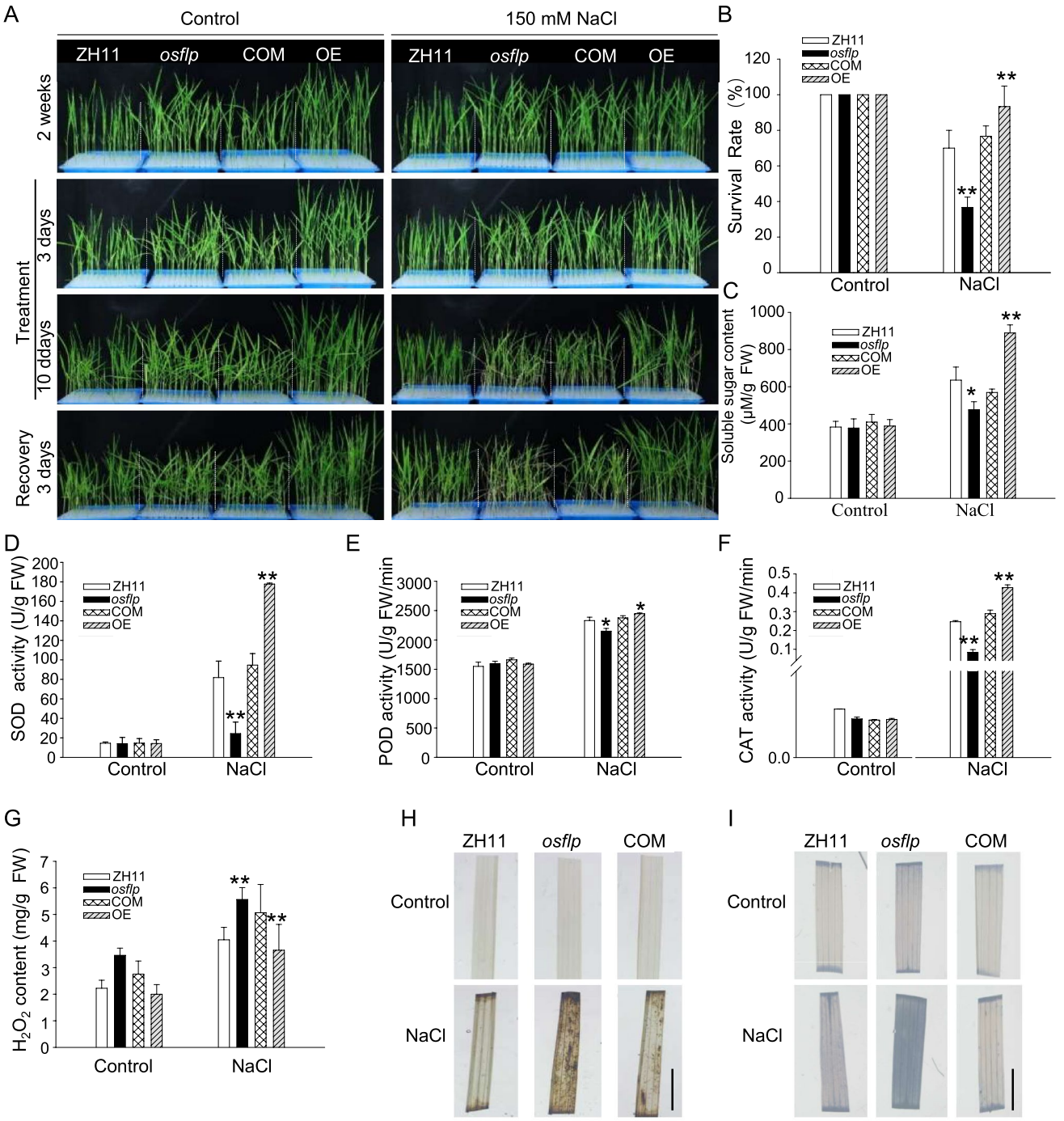

Fig. 4 More ROS was accumulated in *osflp* rice mutant under salt stress conditions. **A** Salt stress phenotype assay of ZH11, *osflp*, COM, and OE seedlings cultivated with hydroponic culture. Two-week-old seedlings were treated with or without 150 mM NaCl in hydroponic culture after 3 days, 10 days, and 3 days of restored growth. **B** Survival rate was analyzed after 3 days of recovery. **C** Soluble sugar content was measured after 3 days of recovery. **D–G** SOD activity (**D**), POD activity (**E**), CAT activity (**F**), and H_2O_2 content (**G**) were assayed after 3 days of recovery. Data are means ± SD from three biological replicates. Student's *t*-test was performed. Statistically significant differences are indicated with asterisks: $*P < 0.05$, $**P < 0.01$. Both DAB (**H**) and NBT (**I**) staining showed more ROS accumulation in *osflp* mutant leaves treated with 150 mM NaCl treatment after 24 h. Scale bars = 0.5 cm

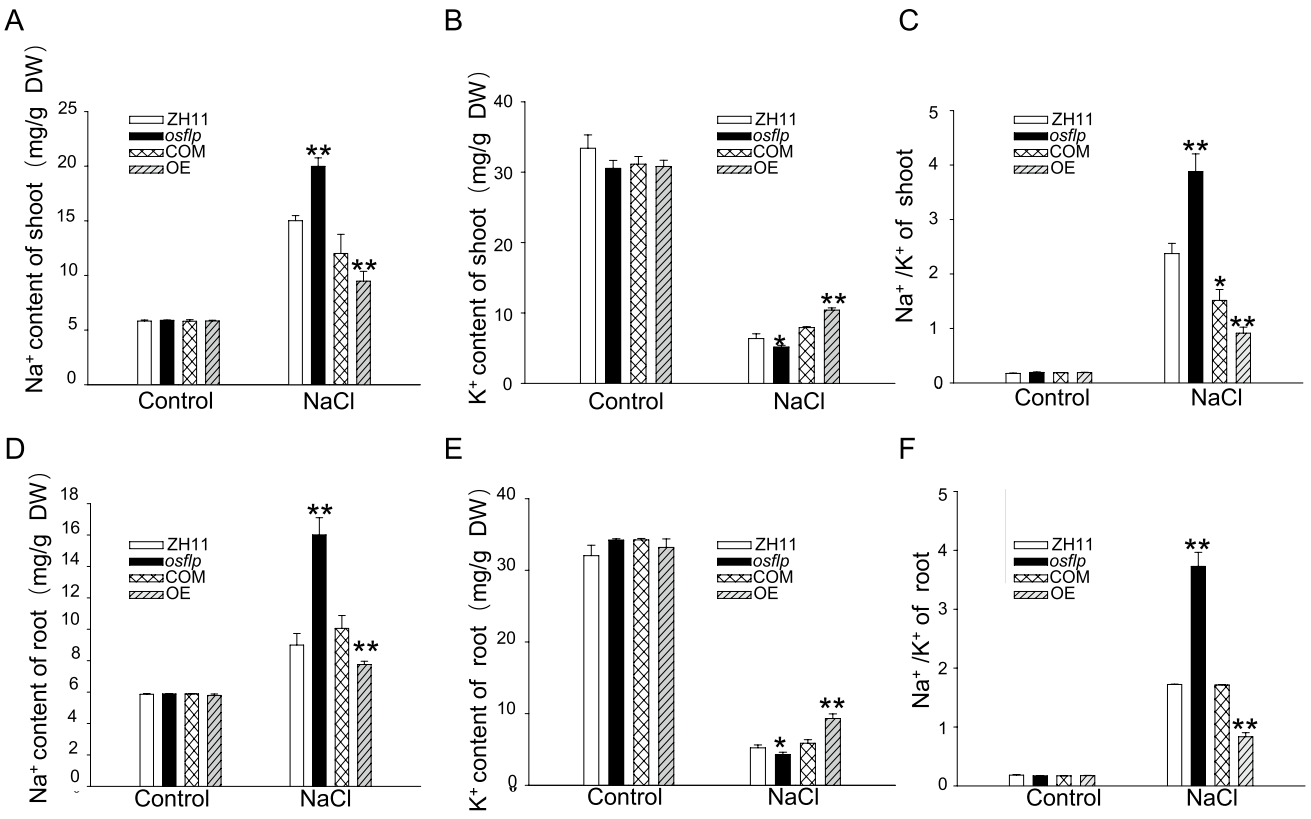

Fig. 5 *osflp* mutant accumulates more Na^+ and less K^+ in shoots and roots under salt stress Na^+ and K^+ contents assay in root and shoot of ZH11, *osflp*, COM and OE lines of rice plants. Two-week-old seedlings were treated with or without 150 mM NaCl for 4 days. **A**, **B** Na^+ and K^+ contents were measured in the shoot. **C** The ratio of Na^+ to K^+ in the shoot was calculated according to the measurements in (**A**, **B**). **D**, **E** Na^+ and K^+ contents were measured in root. **F** The ratio of Na^+ to K^+ in root was calculated according to the measurements in (**D**, **E**). Data are means ± SD from three biological replicates. The student's t-test was performed. Statistically, significant differences were indicated with asterisks: *$p < 0.05$, **$p < 0.01$

binds to the promoter region of *OsCDKB1;1* and represses the expression of *OsCDKB1;1* leading to a decrease in the ROS accumulation resulting in salt tolerance in rice. In *osflp* mutant plant, the expression of *OsCDKB1;1* is activated and the ROS accumulation is increased, ultimately, enhancing salt sensitivity in rice. Together, our findings extend the knowledge about the role of OsFLP in rice, especially in salt stress response, indicating the potential benefits for the improvement of salt-tolerant rice cultivar.

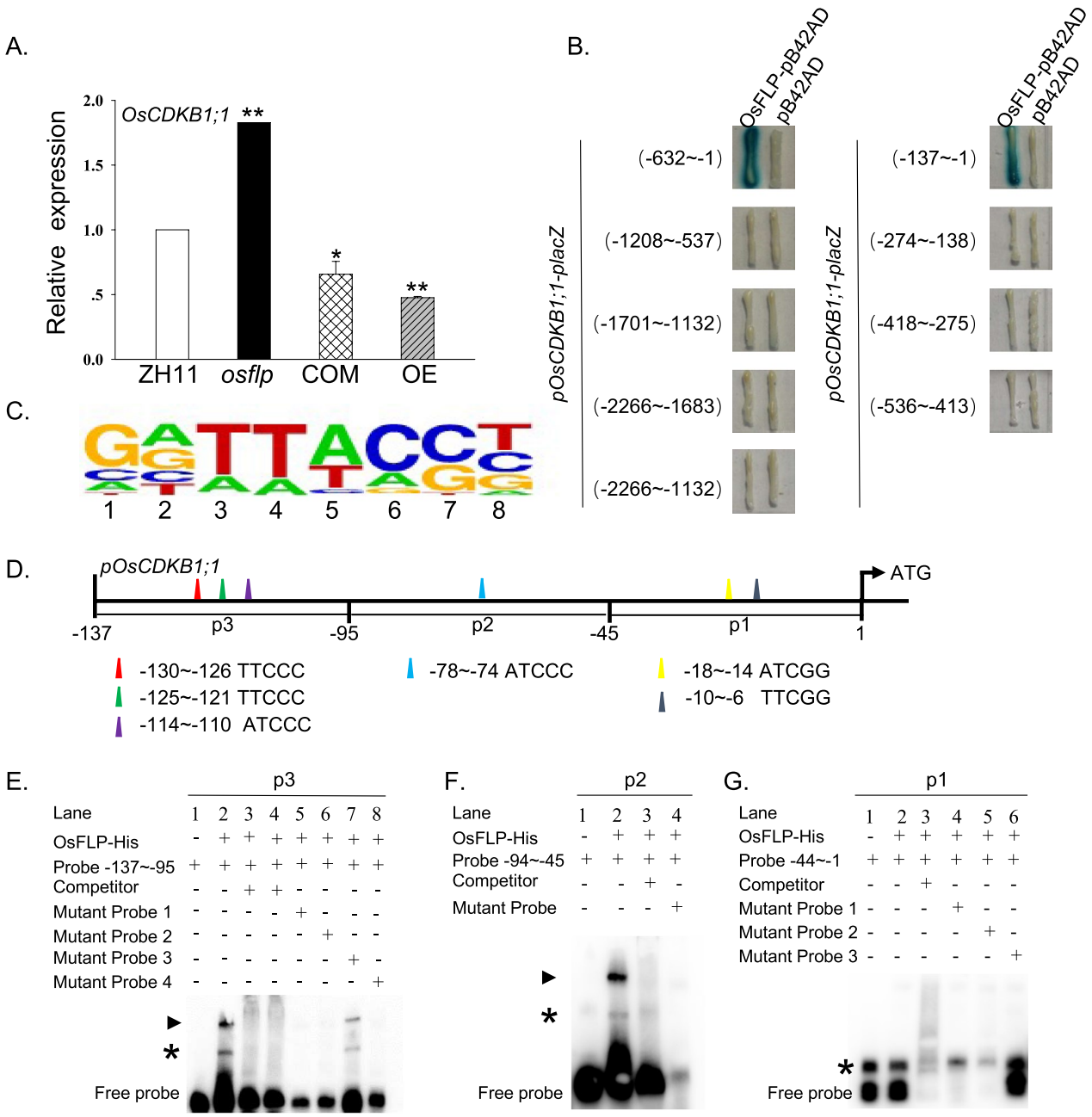

Fig. 6 OsFLP directly binds to the promoter region of *OsCDKB1:1* and regulates its transcriptional expression. **A** The transcriptional expression of *OsCDKB1;1* was negatively regulated by OsFLP. The transcriptional level of *OsCDKB1;1* was detected by RT-qPCR in ZH11, *osflp*, COM, and OE lines of rice plants. **B** OsFLP binds to the promoter region *of OsCDKB1;1* in yeast one-hybrid assay. The full length of the promoter region of *OsCDKB1;1* was truncated into nine fragments. The area from -137 bp to − 1 bp was identified as the minimal promoter region, which is the region for the binding of OsFLP. **C** High scoring consensus sequence which might be the targeting site of OsFLP was identified by ChIP-seq analysis. **D** Schematic diagram of *OsCDKB1;1* promoter region showing potential binding sites of OsFLP in three different regions including P1, P2, and P3. **E–H** Electrophoretic mobility shift assays (EMSA) indicated OsFLP specifically bound to the promoter region of the *OsCDKB1;1*. The arrows indicate the protein-DNA complexes. The asterisks indicate the non-specific binding. The competitor was the probe without biotin label

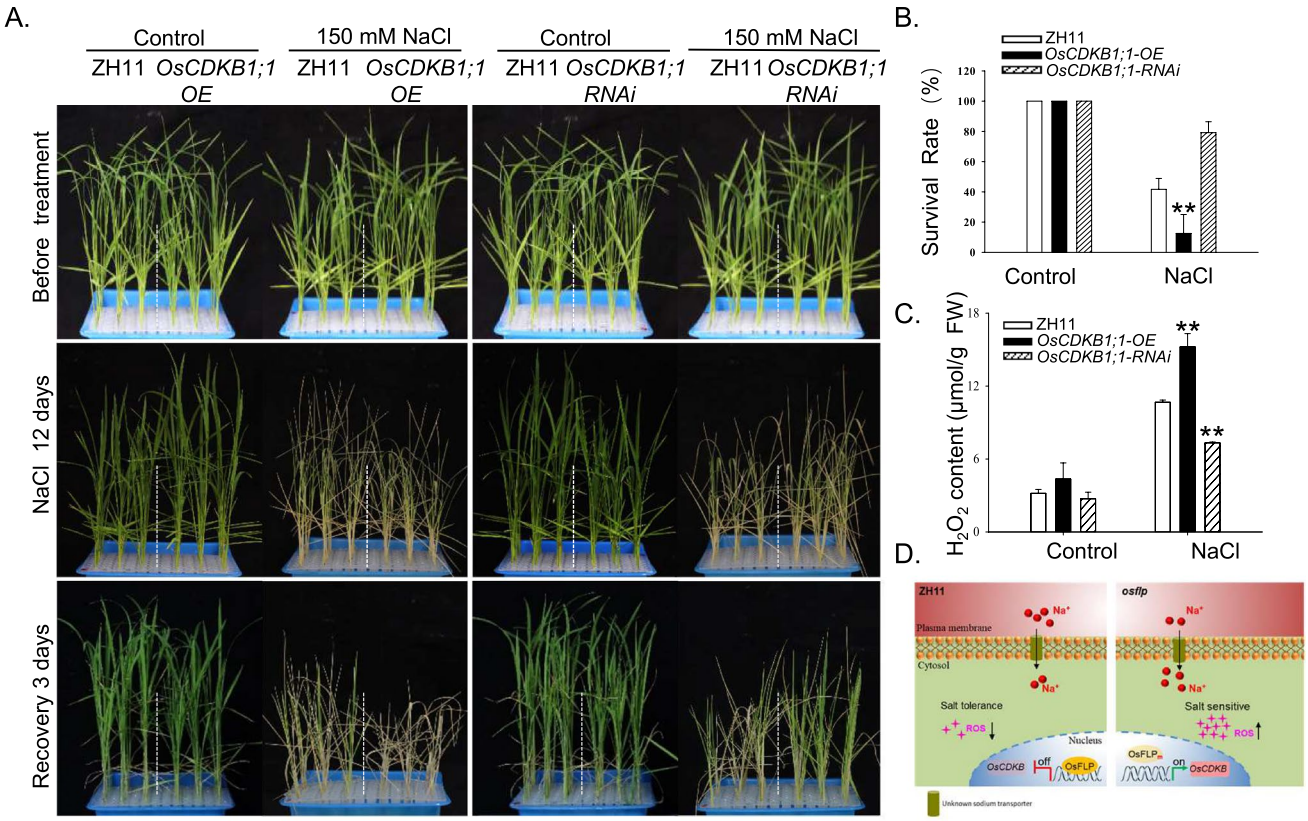

Fig. 7 *OsCDKB1;1* negatively regulates the response to salt stress in rice. **A** Salt stress phenotype analysis of ZH11, *OsCDKB1;1*-OE, *OsCDKB1;1*-RNAi. Two-week-old seedlings were cultivated in hydroponic culture with or without 150 mM NaCl for 12 days and then restored growth for 3 days. **B** The survival rates of ZH11, *OsCDKB1;1*-OE, *OsCDKB1;1*-RNAi were analyzed after salt stress recovery. **C** The content of H_2O_2 was monitored in ZH11, *OsCDKB1;1*-OE, *OsCDKB1;1*-RNAi after salt stress recovery. Data in (**B** and **C**) are means ± SD from three biological replicates. The student's *t-test* was performed. Statistically, significant differences are indicated with asterisks: $^{**}P < 0.01$. **D** Proposed working model for OsFLP-*OsCDKB1;1* transcriptional regulation module mediated salt stress response in rice. Under salt stress conditions, in ZH11, OsFLP binds to the promoter region of *OsCDKB1;1* to repress the transcriptional expression of *OsCDKB1;1* resulting in less ROS accumulation, ultimately conferring salt tolerance (in the left panel). However, in *osflp* mutant plants, the expression of *OsCDKB1;1* is enhanced, and promotes the ROS accumulation in plants, thereby leading to salt sensitivity in rice (in the right panel). $OsFLP_m$ indicates mutation of OsFLP

Supplementary Information The online version contains supplementary material available at https://doi.org/10.1007/s11103-022-01282-9.

Acknowledgements We would like to thank Dr. Prabha Manishankar (University of Tübingen, Germany) for helpful comments and critical reading. This work was supported by grants from the Strategic Priority Research Program of the Chinese Academy of Sciences (Grant No. XDA24010303) and the National Natural Science Foundation of China (Grant Nos. 31970804 and 32170722 to J. L, Grant No. 31470362 to J.-J. Z and Grant Nos. 31871377 and 32070723 to K.-Z. Y).

Author contributions C.-X. Z and J. Z performed the experiments and analyzed the data. H.-C. L, X.-X. Q, J.-X. W, Q.-X.-M. H and J.-J. Z participated in parts of experiments and data analysis. J. L, K.-Z. Y, C.-X. Z and J. Z designed the experiments. C.-X. Z and J. L wrote the manuscript. All authors read and approved the final manuscript.

Funding This work was supported by grants from the Strategic Priority Research Program of the Chinese Academy of Sciences (Grant No. XDA24010303) and the National Natural Science Foundation of China (Grant Nos. 31970804 and 32170722 to J. L, Grant Nos. 31470362 to J.-J. Z. and Grant Nos. 31871377 and 32070723 to K.-Z. Y.).

Data availability All data generated during this study are included in this published article and its supplementary information files. The RNA-seq datasets generated during the current study are available in the NCBI Sequence Read Archive (SRA) repository, https://dataview.ncbi.nlm.nih.gov/object/PRJNA805061?reviewer=m847fdbhc5h8hlajg783fodski The ChIP-seq datasets generated during the current study are available in the NCBI Sequence Read Archive (SRA) repository, https://dataview.ncbi.nlm.nih.gov/object/PRJNA803610?reviewer=8ark21mh1c3mrblaoj1fnpek34.

Declarations

Conflict of interest The authors have no relevant financial or non-financial interest to disclose.

References

Almagro L, Gómez Ros LV, Belchi-Navarro S, Bru R, Ros Barceló A, Pedreño MA (2009) Class III peroxidases in plant defence reactions. J Exp Bot 60:377–390. https://doi.org/10.1093/jxb/ern277

Andersen SU, Buechel S, Zhao Z, Ljung K, Novák O, Busch W, Schuster C, Lohmann JU (2008) Requirement of B2-type cyclin-dependent kinases for meristem integrity in *Arabidopsis thaliana*. Plant Cell 20:88–100. https://doi.org/10.1105/tpc.107.054676

Bhatt I, Tripathi BN (2011) Plant peroxiredoxins: catalytic mechanisms, functional significance and future perspectives. Biotechnol Adv 29:850–859. https://doi.org/10.1016/j.biotechadv.2011.07.002

Boudolf V, Rombauts S, Naudts M, Inzé D, De Veylder L (2001) Identification of novel cyclin-dependent kinases interacting with the CKS1 protein of Arabidopsis. J Exp Bot 52:1381–1382. https://doi.org/10.1093/jexbot/52.359.1381

Burssens S, Himanen K, van de Cotte B, Beeckman T, Van Montagu M, Inzé D, Verbruggen N (2000) Expression of cell cycle regulatory genes and morphological alterations in response to salt stress in *Arabidopsis thaliana*. Planta 211:632–640. https://doi.org/10.1007/s004250000334

Chen T, Shabala S, Niu Y, Chen Z-H, Shabala L, Meinke H, Venkataraman G, Pareek A, Xu J, Zhou M (2021) Molecular mechanisms of salinity tolerance in rice. Crop J 9:506–520. https://doi.org/10.1016/j.cj.2021.03.005

De Veylder L, Joubès J, Inzé D (2003) Plant cell cycle transitions. Curr Opin Plant Biol 6:536–543. https://doi.org/10.1016/j.pbi.2003.09.001

Dewitte W, Murray JA (2003) The plant cell cycle. Annu Rev Plant Biol 54:235–264. https://doi.org/10.1146/annurev.arplant.54.031902.134836

Dubos C, Stracke R, Grotewold E, Weisshaar B, Martin C, Lepiniec L (2010) MYB transcription factors in Arabidopsis. Trends Plant Sci 15:573–581. https://doi.org/10.1016/j.tplants.2010.06.005

Dubey RS, Singh AK (1999) Salinity induces accumulation of soluble sugars and alters the activity of sugar metabolizing enzymes in rice plants. Biol Plant 42:233–239. https://doi.org/10.1023/A:1002160618700

El-Kereamy A, Bi YM, Ranathunge K, Beatty PH, Good AG, Rothstein SJ (2012) The rice R2R3-MYB transcription factor OsMYB55 is involved in the tolerance to high temperature and modulates amino acid metabolism. PLoS One 7:e52030. https://doi.org/10.1371/journal.pone.0052030

Gray JE, Holroyd GH, van der Lee FM, Bahrami AR, Sijmons PC, Woodward FI, Schuch W, Hetherington AM (2000) The HIC signalling pathway links CO_2 perception to stomatal development. Nature 408:713–716. https://doi.org/10.1038/35047071

Gupta B, Huang B (2014) Mechanism of salinity tolerance in plants: physiological, biochemical, and molecular characterization. Int J Genomics 2014:701596. https://doi.org/10.1155/2014/701596

Hasanuzzaman M, Raihan MRH, Masud AAC, Rahman K, Nowroz F, Rahman M, Nahar K, Fujita M (2021) Regulation of reactive oxygen species and antioxidant defense in plants under salinity. Int J Mol Sci. https://doi.org/10.3390/ijms22179326

Hiei Y, Ohta S, Komari T, Kumashiro T (1994) Efficient transformation of rice (*Oryza sativa* L.) mediated by Agrobacterium and sequence analysis of the boundaries of the T-DNA. Plant J 6:271–282. https://doi.org/10.1046/j.1365-313x.1994.6020271.x

Horie T, Yoshida K, Nakayama H, Yamada K, Oiki S, Shinmyo A (2001) Two types of HKT transporters with different properties of Na^+ and K^+ transport in *Oryza sativa*. Plant J 27:129–138. https://doi.org/10.1046/j.1365-313x.2001.01077.x

James RA, Blake C, Byrt CS, Munns R (2011) Major genes for Na^+ exclusion, Nax1 and Nax2 (wheat HKT1;4 and HKT1;5), decrease Na^+ accumulation in bread wheat leaves under saline and waterlogged conditions. J Exp Bot 62:2939–2947. https://doi.org/10.1093/jxb/err003

Kanaoka MM, Pillitteri LJ, Fujii H, Yoshida Y, Bogenschutz NL, Takabayashi J, Zhu JK, Torii KU (2008) SCREAM/ICE1 and SCREAM2 specify three cell-state transitional steps leading to Arabidopsis stomatal differentiation. Plant Cell 20:1775–1785. https://doi.org/10.1105/tpc.108.060848

Kreps JA, Wu Y, Chang HS, Zhu T, Wang X, Harper JF (2002) Transcriptome changes for Arabidopsis in response to salt, osmotic, and cold stress. Plant Physiol 130:2129–2141. https://doi.org/10.1104/pp.008532

Koevoets IT, Venema JH, Elzenga JTM, Testerink C (2016) Roots withstanding their environment: exploiting root system architecture responses to abiotic stress to improve crop tolerance. Front Plant Sci 7:1335

Korver RA, Koevoets IT, Testerink C (2018) Out of shape during stress: a key role for auxin. Trends Plant Sci 23:783–793

Lai LB, Nadeau JA, Lucas J, Lee EK, Nakagawa T, Zhao L, Geisler M, Sack FD (2005) The Arabidopsis R2R3 MYB proteins FOUR LIPS and MYB88 restrict divisions late in the stomatal cell lineage. Plant Cell 17:2754–2767. https://doi.org/10.1105/tpc.105.034116

Lei Q, Lee E, Keerthisinghe S, Lai L, Li M, Lucas JR, Wen X, Ren X, Sack FD (2015) The FOUR LIPS and MYB88 transcription factor genes are widely expressed in *Arabidopsis thaliana* during development. Am J Bot 102:1521–1528. https://doi.org/10.3732/ajb.1500056

Lv Y, Yang M, Hu D, Yang Z, Ma S, Li X, Xiong L (2017) The OsMYB30 transcription factor suppresses cold tolerance by interacting with a JAZ protein and suppressing β-amylase expression. Plant Physiol 173:1475–1491. https://doi.org/10.1104/pp.16.01725

Mahapatra K, Roy S (2021) SOG1 transcription factor promotes the onset of endoreduplication under salinity stress in Arabidopsis. Sci Rep 11:11659. https://doi.org/10.1038/s41598-021-91293-1

Mäkelä P, Kontturi M, Pehu E, Somersalo S (1999) Photosynthetic response of drought- and salt-stressed tomato and turnip rape plants to foliar-applied glycinebetaine. Physiol Plant 105:45–50. https://doi.org/10.1034/j.1399-3054.1999.105108.x

Makkena S, Lee E, Sack FD, Lamb RS (2012) The R2R3 MYB transcription factors FOUR LIPS and MYB88 regulate female reproductive development. J Exp Bot 63:5545–5558. https://doi.org/10.1093/jxb/ers209

Martin C, Paz-Ares J (1997) MYB transcription factors in plants. Trends Genet 13:67–73. https://doi.org/10.1016/s0168-9525(96)10049-4

Matsui A, Ishida J, Morosawa T, Mochizuki Y, Kaminuma E, Endo TA, Okamoto M, Nambara E, Nakajima M, Kawashima M, Satou M, Kim JM, Kobayashi N, Toyoda T, Shinozaki K, Seki M (2008) Arabidopsis transcriptome analysis under drought, cold, high-salinity and ABA treatment conditions using a tiling array. Plant Cell Physiol 49:1135–1149. https://doi.org/10.1093/pcp/pcn101

Menges M, de Jager SM, Gruissem W, Murray JA (2005) Global analysis of the core cell cycle regulators of Arabidopsis identifies novel genes, reveals multiple and highly specific profiles of expression and provides a coherent model for plant cell cycle control. Plant J 41:546–566. https://doi.org/10.1111/j.1365-313X.2004.02319.x

Miao BH, Han XG, Zhang WH (2010) The ameliorative effect of silicon on soybean seedlings grown in potassium-deficient medium. Ann Bot 105:967–973. https://doi.org/10.1093/aob/mcq063

Miller G, Suzuki N, Ciftci-Yilmaz S, Mittler R (2010) Reactive oxygen species homeostasis and signalling during drought and salinity

stresses. Plant Cell Environ 33:453–467. https://doi.org/10.1111/j.1365-3040.2009.02041.x
Mittler R (2002) Oxidative stress, antioxidants and stress tolerance. Trends Plant Sci 7:405–410. https://doi.org/10.1016/s1360-1385(02)02312-9
Mittler R, Vanderauwera S, Gollery M, Van Breusegem F (2004) Reactive oxygen gene network of plants. Trends Plant Sci 9:490–498. https://doi.org/10.1016/j.tplants.2004.08.009
Noctor G, Foyer CH (1998) ASCORBATE AND GLUTATHIONE: keeping active oxygen under control. Annu Rev Plant Physiol Plant Mol Biol 49:249–279. https://doi.org/10.1146/annurev.arplant.49.1.249
Ponce KS, Meng L, Guo L, Leng Y, Ye G (2021) Advances in sensing, response and regulation mechanism of salt tolerance in rice. Int J Mol Sci. https://doi.org/10.3390/ijms22052254
Porceddu A, Stals H, Reichheld JP, Segers G, De Veylder L, Barroco RP, Casteels P, Van Montagu M, Inzé D, Mironov V (2001) A plant-specific cyclin-dependent kinase is involved in the control of G2/M progression in plants. J Biol Chem 276:36354–36360. https://doi.org/10.1074/jbc.M011060200
Qu X, Yan M, Zou J, Jiang M, Yang K, Le J (2018) A2-type cyclin is required for the asymmetric entry division in rice stomatal development. J Exp Bot 69:3587–3599. https://doi.org/10.1093/jxb/ery158
Roy SJ, Negrão S, Tester M (2014) Salt resistant crop plants. Curr Opin Biotechnol 26:115–124. https://doi.org/10.1016/j.copbio.2013.12.004
Shen H, Zhong X, Zhao F, Wang Y, Yan B, Li Q, Chen G, Mao B, Wang J, Li Y, Xiao G, He Y, Xiao H, Li J, He Z (2015a) Overexpression of receptor-like kinase ERECTA improves thermotolerance in rice and tomato. Nat Biotechnol 33:996–1003. https://doi.org/10.1038/nbt.3321
Shen Y, Shen L, Shen Z, Jing W, Ge H, Zhao J, Zhang W (2015b) The potassium transporter OsHAK21 functions in the maintenance of ion homeostasis and tolerance to salt stress in rice. Plant Cell Environ 38:2766–2779. https://doi.org/10.1111/pce.12586
Shpak ED, McAbee JM, Pillitteri LJ, Torii KU (2005) Stomatal patterning and differentiation by synergistic interactions of receptor kinases. Science 309:290–293. https://doi.org/10.1126/science.1109710
Song SY, Chen Y, Chen J, Dai XY, Zhang WH (2011) Physiological mechanisms underlying OsNAC5-dependent tolerance of rice plants to abiotic stress. Planta 234:331–345. https://doi.org/10.1007/s00425-011-1403-2
Tang L, Cai H, Ji W, Luo X, Wang Z, Wu J, Wang X, Cui L, Wang Y, Zhu Y, Bai X (2013) Overexpression of GsZFP1 enhances salt and drought tolerance in transgenic alfalfa (*Medicago sativa* L.). Plant Physiol Biochem 71:22–30. https://doi.org/10.1016/j.plaphy.2013.06.024
Vandepoele K, Raes J, De Veylder L, Rouzé P, Rombauts S, Inzé D (2002) Genome-wide analysis of core cell cycle genes in Arabidopsis. Plant Cell 14:903–916. https://doi.org/10.1105/tpc.010445
Wang HZ, Yang KZ, Zou JJ, Zhu LL, Xie ZD, Morita MT, Tasaka M, Friml J, Grotewold E, Beeckman T, Vanneste S, Sack F, Le J (2015) Transcriptional regulation of PIN genes by FOUR LIPS and MYB88 during Arabidopsis root gravitropism. Nat Commun 6:8822. https://doi.org/10.1038/ncomms9822
Wang X, Niu Y, Zheng Y (2021) Multiple functions of MYB transcription factors in abiotic stress responses. Int J Mol Sci. https://doi.org/10.3390/ijms22116125
West G, Inzé D, Beemster GT (2004) Cell cycle modulation in the response of the primary root of Arabidopsis to salt stress. Plant Physiol 135:1050–1058. https://doi.org/10.1104/pp.104.040022
Wu Z, Chen L, Yu Q, Zhou W, Gou X, Li J, Hou S (2019) Multiple transcriptional factors control stomata development in rice. New Phytol 223:220–232. https://doi.org/10.1111/nph.15766
Xia XJ, Gao CJ, Song LX, Zhou YH, Shi K, Yu JQ (2014) Role of H2O2 dynamics in brassinosteroid-induced stomatal closure and opening in Solanum lycopersicum. Plant Cell Environ 37:2036–2050. https://doi.org/10.1111/pce.12275
Xie Z, Lee E, Lucas JR, Morohashi K, Li D, Murray JA, Sack FD, Grotewold E (2010a) Regulation of cell proliferation in the stomatal lineage by the Arabidopsis MYB FOUR LIPS via direct targeting of core cell cycle genes. Plant Cell 22:2306–2321. https://doi.org/10.1105/tpc.110.074609
Xie Z, Li D, Wang L, Sack FD, Grotewold E (2010b) Role of the stomatal development regulators FLP/MYB88 in abiotic stress responses. Plant J 64:731–739. https://doi.org/10.1111/j.1365-313X.2010b.04364.x
Xiong L, Schumaker KS, Zhu JK (2002) Cell signaling during cold, drought, and salt stress. Plant Cell 14(Suppl):S165-183. https://doi.org/10.1105/tpc.000596
Yang A, Dai X, Zhang WH (2012) A R2R3-type MYB gene, OsMYB2, is involved in salt, cold, and dehydration tolerance in rice. J Exp Bot 63:2541–2556. https://doi.org/10.1093/jxb/err431
Yang K, Zhu L, Wang H, Jiang M, Xiao C, Hu X, Vanneste S, Dong J, Le J (2019) A conserved but plant-specific CDK-mediated regulation of DNA replication protein A2 in the precise control of stomatal terminal division. Proc Natl Acad Sci USA 116:18126–18131. https://doi.org/10.1073/pnas.1819345116
Yang M, Sack FD (1995) The too many mouths and four lips mutations affect stomatal production in Arabidopsis. Plant Cell 7:2227–2239. https://doi.org/10.1105/tpc.7.12.2227
Yang Y, Guo Y (2018) Unraveling salt stress signaling in plants. J Integr Plant Biol 60:796–804. https://doi.org/10.1111/jipb.12689
Ye Y, Liu B, Zhao M, Wu K, Cheng W, Chen X, Liu Q, Liu Z, Fu X, Wu Y (2015) CEF1/OsMYB103L is involved in GA-mediated regulation of secondary wall biosynthesis in rice. Plant Mol Biol 89:385–401. https://doi.org/10.1007/s11103-015-0376-0
Zhang H, Liu Y, Wen F, Yao D, Wang L, Guo J, Ni L, Zhang A, Tan M, Jiang M (2014) A novel rice C2H2-type zinc finger protein, ZFP36, is a key player involved in abscisic acid-induced antioxidant defence and oxidative stress tolerance in rice. J Exp Bot 65:5795–5809. https://doi.org/10.1093/jxb/eru313
Zhang H, Zhu J, Gong Z, Zhu JK (2022) Abiotic stress responses in plants. Nat Rev Genet 23:104–119. https://doi.org/10.1038/s41576-021-00413-0
Zhu JK (2003) Regulation of ion homeostasis under salt stress. Curr Opin Plant Biol 6:441–445. https://doi.org/10.1016/s1369-5266(03)00085-2